

Electronic Supplementary Information

for

Photoinduced electron doping of single-walled carbon nanotubes based on carboxamide photochemical reactions

*Naoki Tanaka, Taiki Ishii, Itsuki Yamaguchi, Aoi Hamasuna, Tsuyohiko Fujigaya**

Corresponding Author

Tsuyohiko Fujigaya: fujigaya.tsuyohiko.948@m.kyushu-u.ac.jp

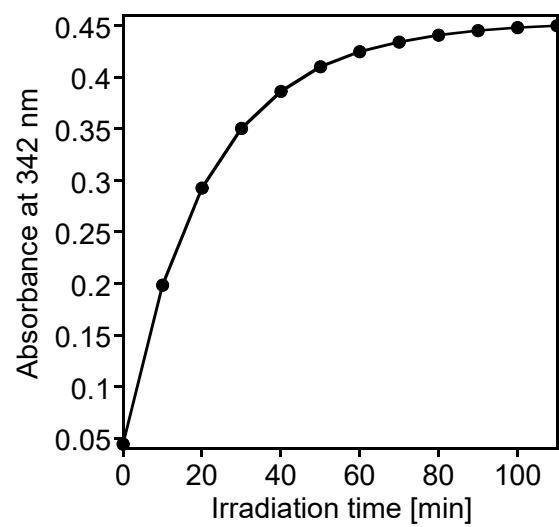


Fig. S1 254-nm UV irradiation time dependency of absorption peak intensities at 342 nm of ethanol solution of N-DMBI-Ox (0.02 mM).

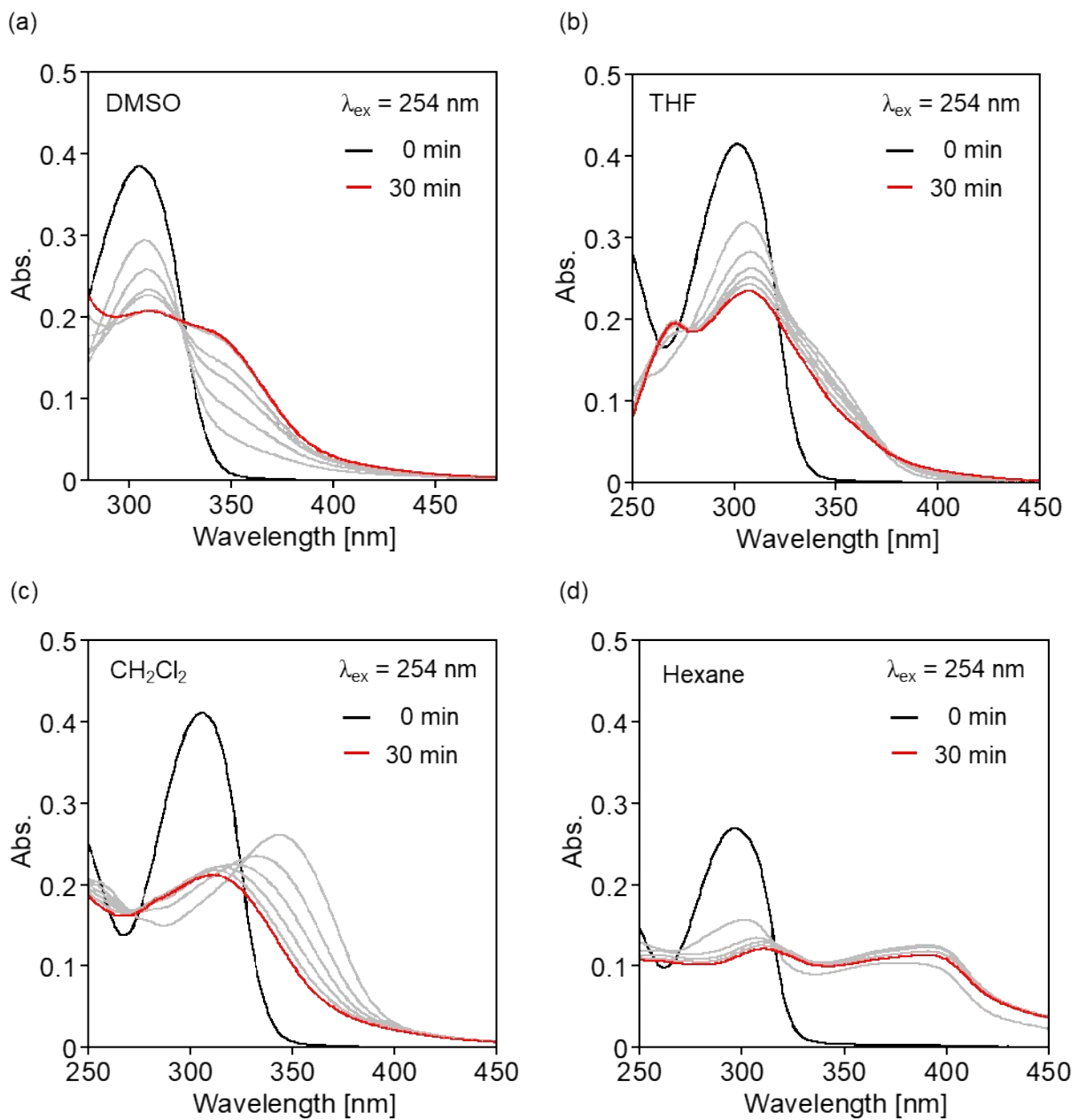


Fig. S2 UV-vis absorption spectra of N-DMBI-Ox after UV irradiation with 254 nm in (a) DMSO (0.02 mM), (b) THF (0.02 mM), (c) CH_2Cl_2 (0.02 mM), and (d) Hexane (0.01 mM).

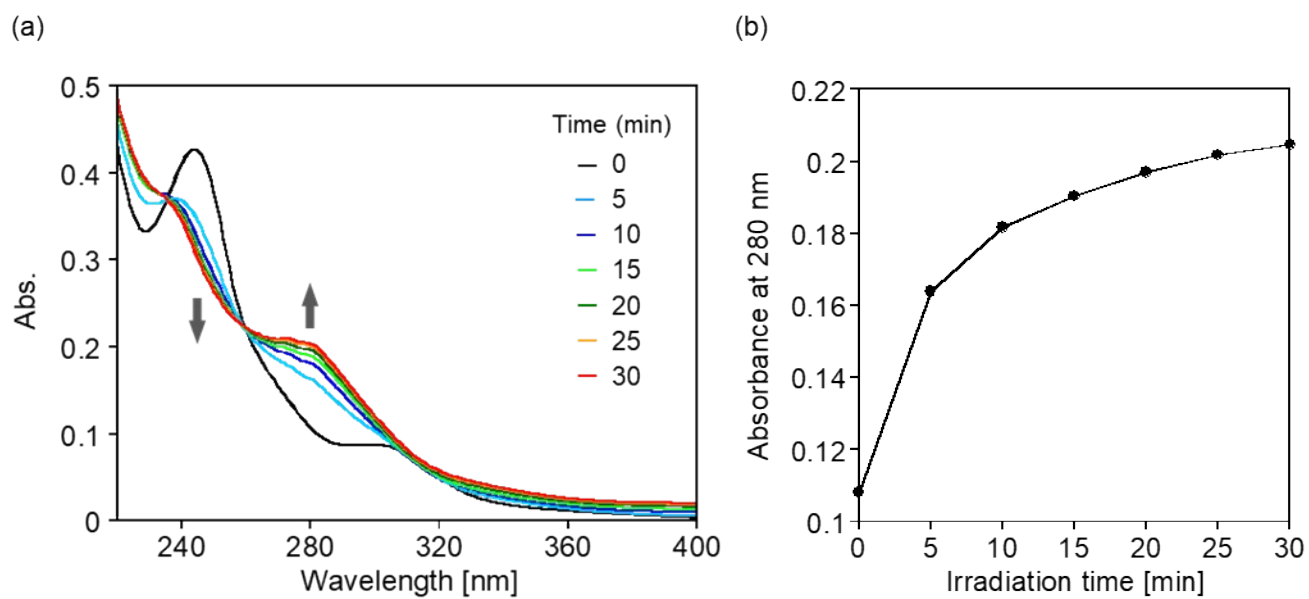


Fig. S3 (a) UV-vis absorption spectra of NO₂-DMBI-Ox in EtOH (0.02 mM) upon UV irradiation. (b) 254-nm UV irradiation time dependency of absorption peak intensities at 280 nm of ethanol solution of NO₂-DMBI-Ox (0.02 mM).

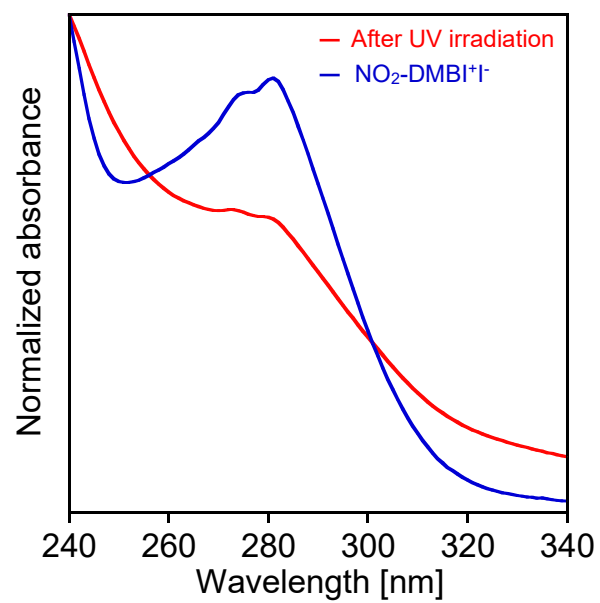


Fig. S4 UV-vis absorption spectra of NO₂-DMBI-Ox (red) after UV irradiation and NO₂-DMBI⁺I⁻ (blue) in EtOH.

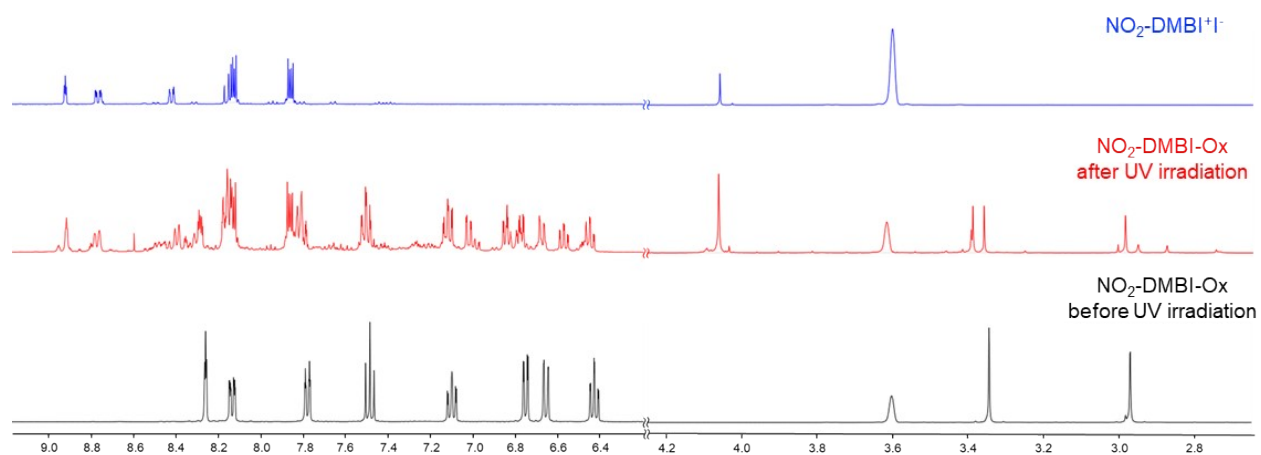


Fig. S5 ^1H NMR spectra of $\text{NO}_2\text{-DMBI}^+\text{I}^-$ (blue) and $\text{NO}_2\text{-DMBI-Ox}$ before (black) and after (red) UV irradiation for 72 hours in $\text{EtOH-}d_3$ solution.

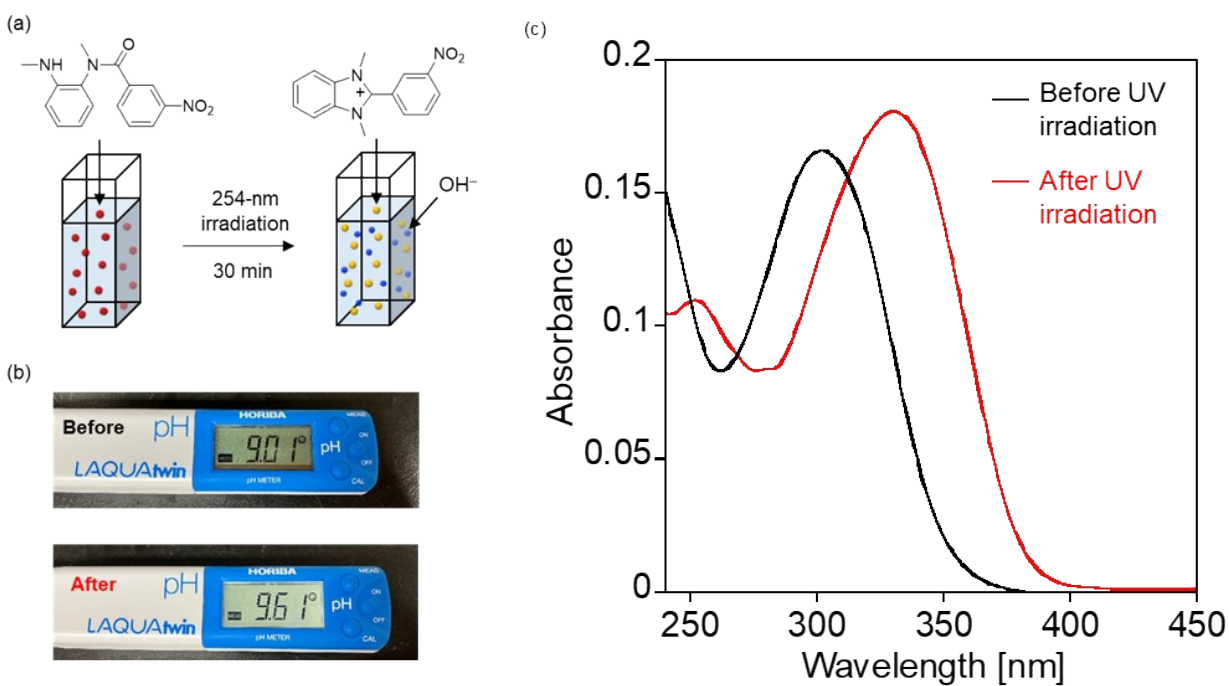


Fig. S6 (a) Schematic illustration of photochemical reaction of NO₂-DMBI-Ox in H₂O and (b) the pH changes of the suspension of NO₂-DMBI-Ox in H₂O before and after UV irradiation. (c) UV-vis absorption spectra of NO₂-DMBI-Ox in H₂O before (black) and after (red) UV irradiation.

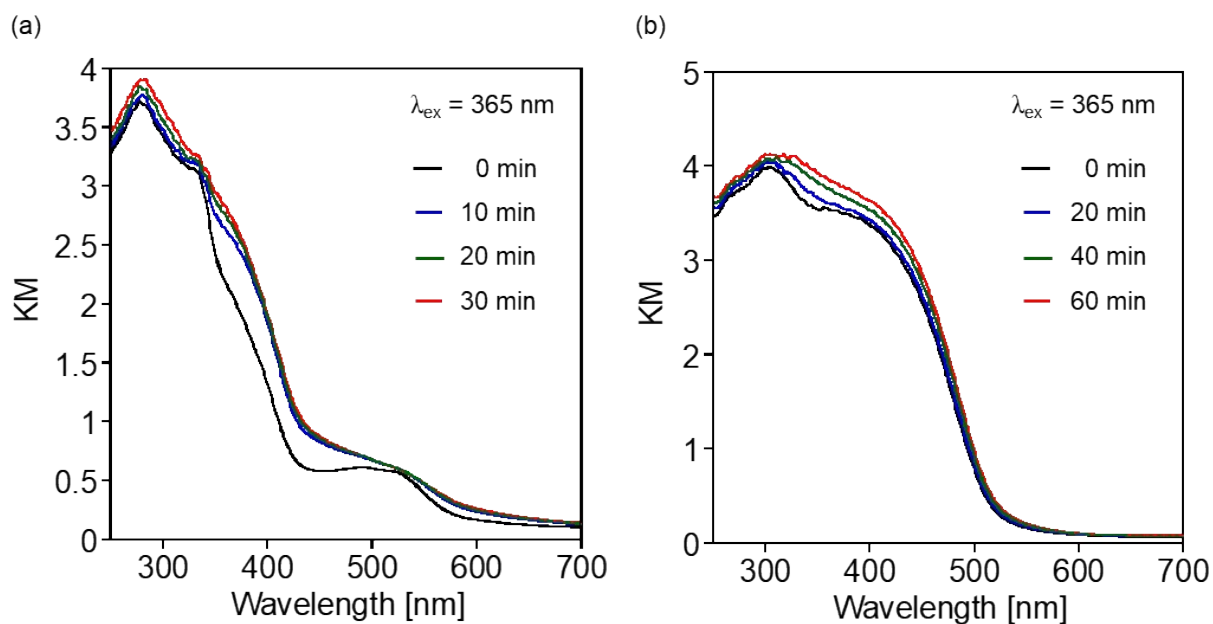


Fig. S7 Diffuse reflectance spectra of (a) N-DMBI-Ox and (b) NO₂-DMBI-Ox upon UV irradiation. The Kubelka-munk function (KM) was calculated based on the kubelka-munk equation ($KM = (1-R)^2/2R$), where R is the relative reflectance of samples using barium sulfate as a standard sample by an integration sphere instrument.

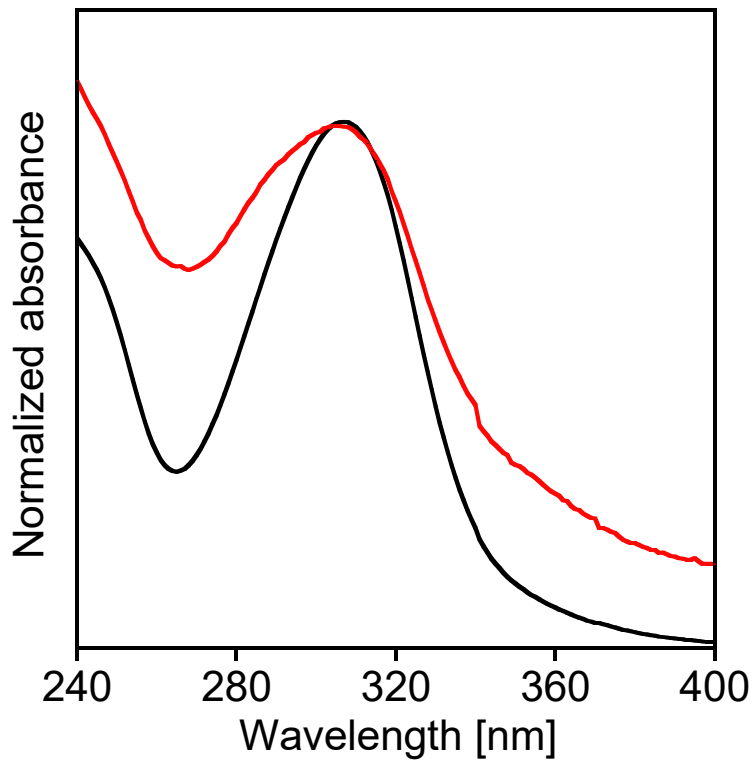


Fig. S8 UV-vis absorption spectra of extracted products (red) from SWCNT sheet after dipping in EtOH solution of N-DMBI-Ox (1.0 mM) and N-DMBI-Ox (black).

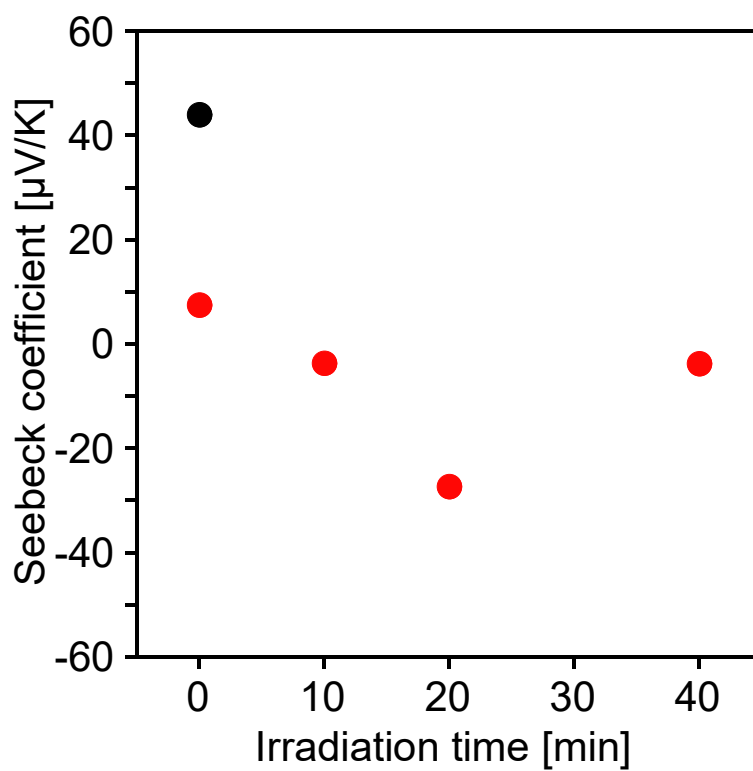


Fig. S9 Irradiation time dependency of Seebeck coefficient of the SWCNT sheets dipped with 1.0 mM of N-DMBI-Ox solutions (red) and pristine SWCNT (black).

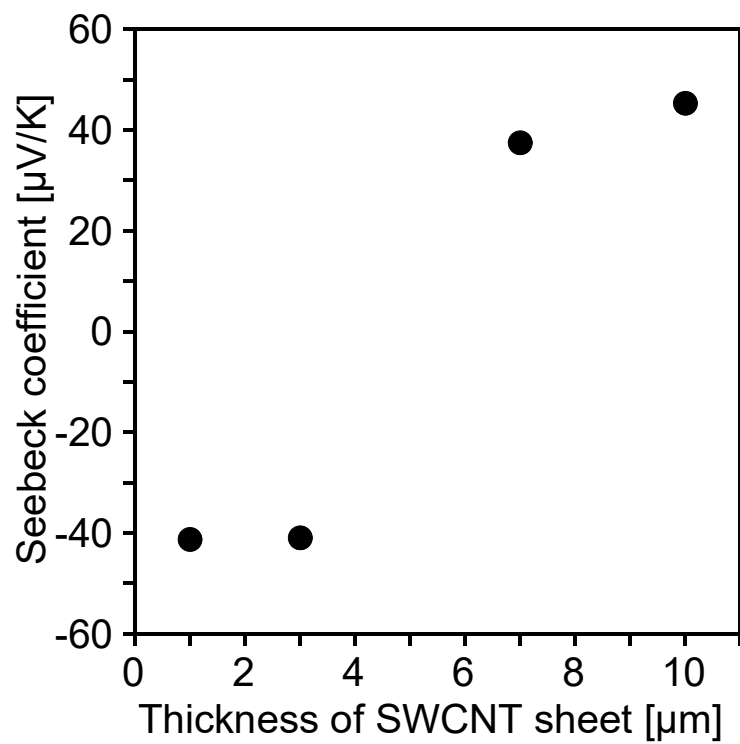


Fig. S10 Thickness dependency of Seebeck coefficient of SWCNT dipped with 1.0 mM of NO_2^- -DMBI-Ox solutions after UV irradiation at 365 nm for 20 min.

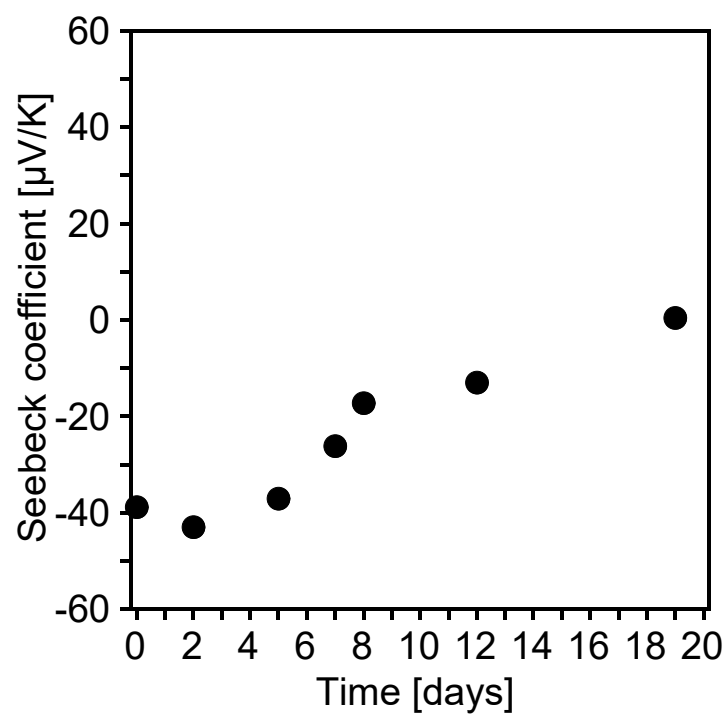


Fig. S11 Time course of the Seebeck coefficient of SWCNT sheets dipped with 1.0 mM of NO_2^- -DMBI-Ox solutions after UV irradiation at 365 nm for 20 min.

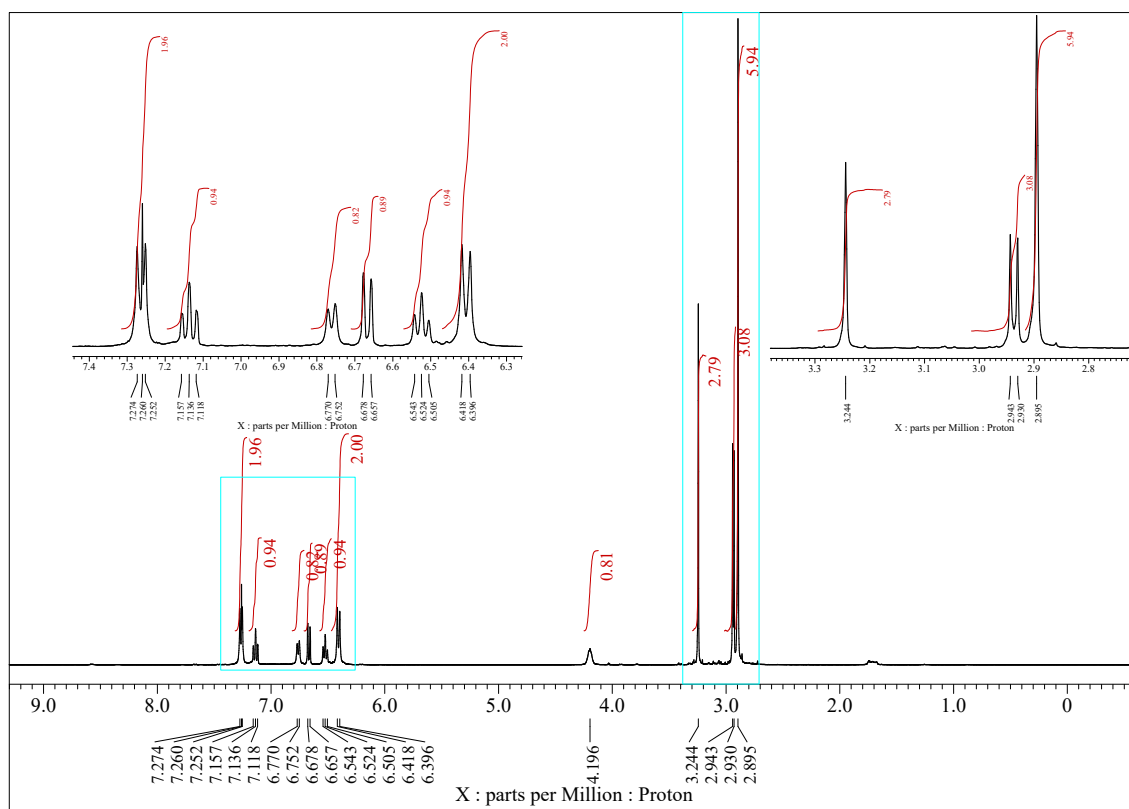


Fig. S12 ^1H NMR spectrum of N-DMBI-Ox (400 MHz, CDCl_3 , 25 $^\circ\text{C}$).

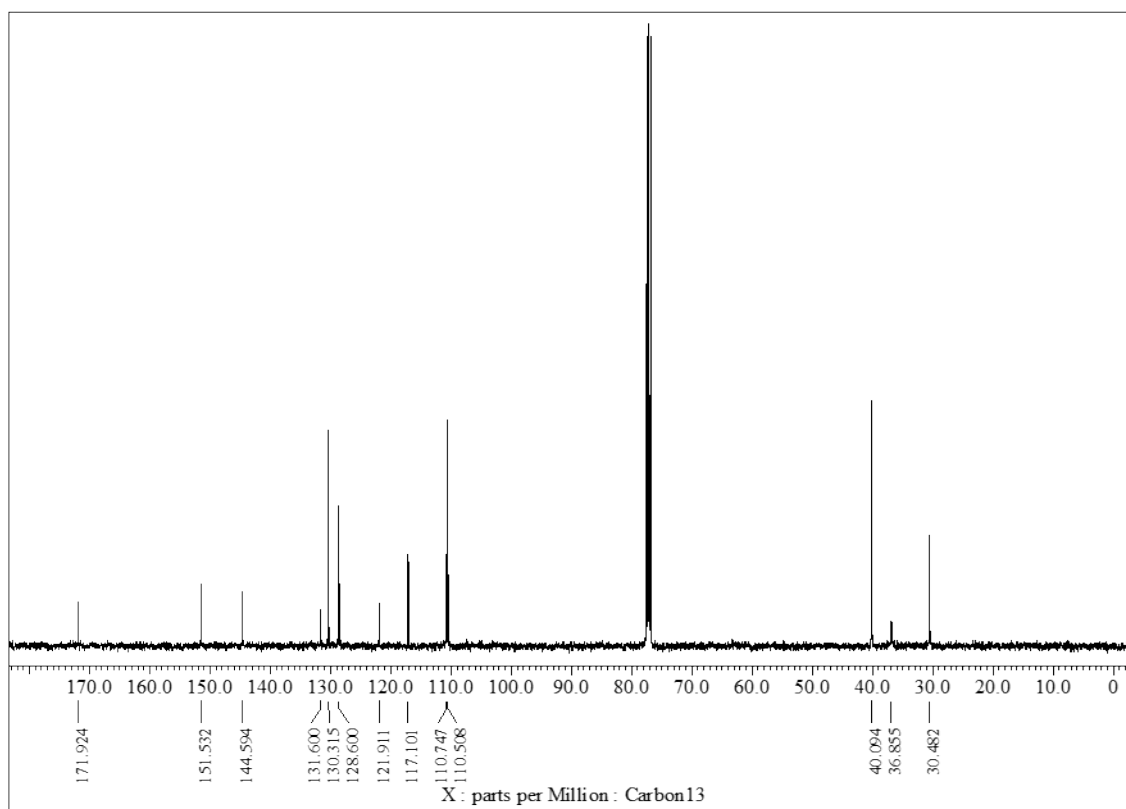


Fig. S13 ^{13}C NMR spectrum of N-DMBI-Ox (100 MHz, CDCl_3 , 25 °C).

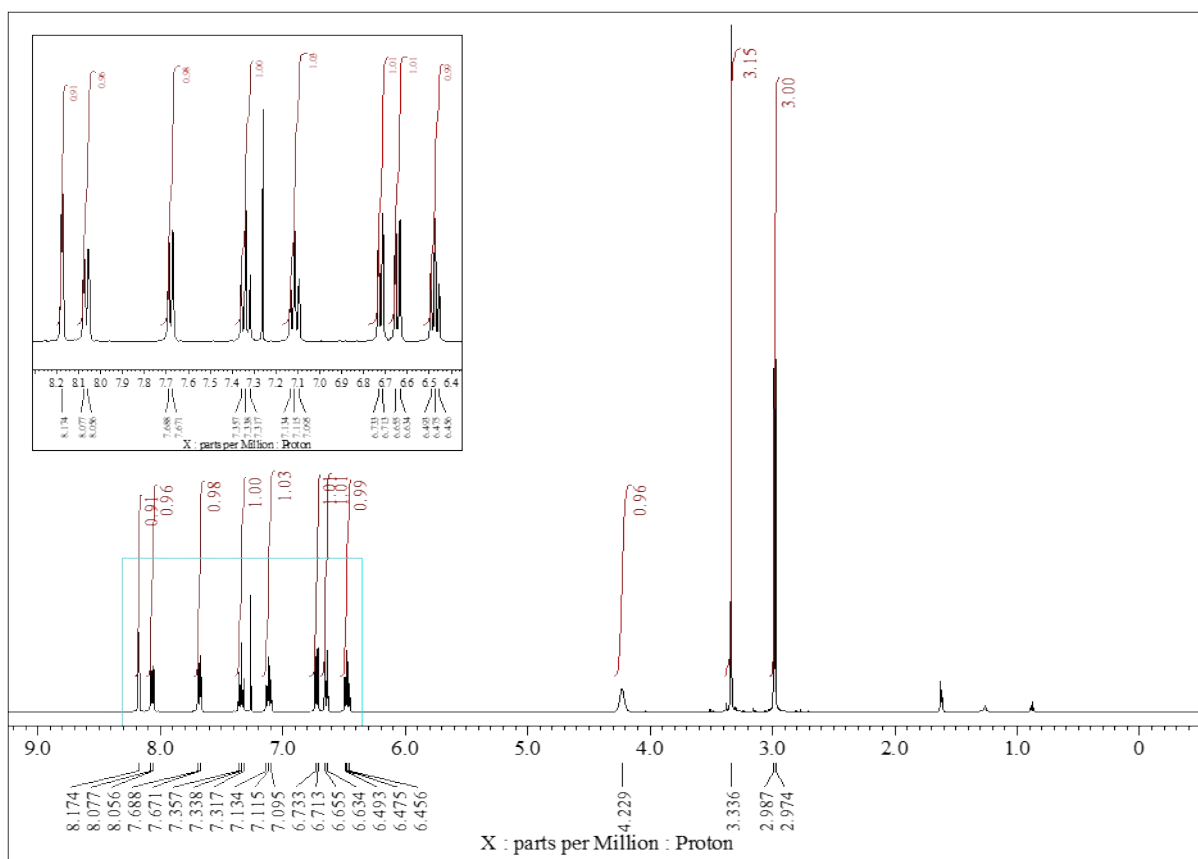


Fig. S14 ^1H NMR spectrum of $\text{NO}_2\text{-DMBI-Ox}$ (400 MHz, CDCl_3 , 25°C).

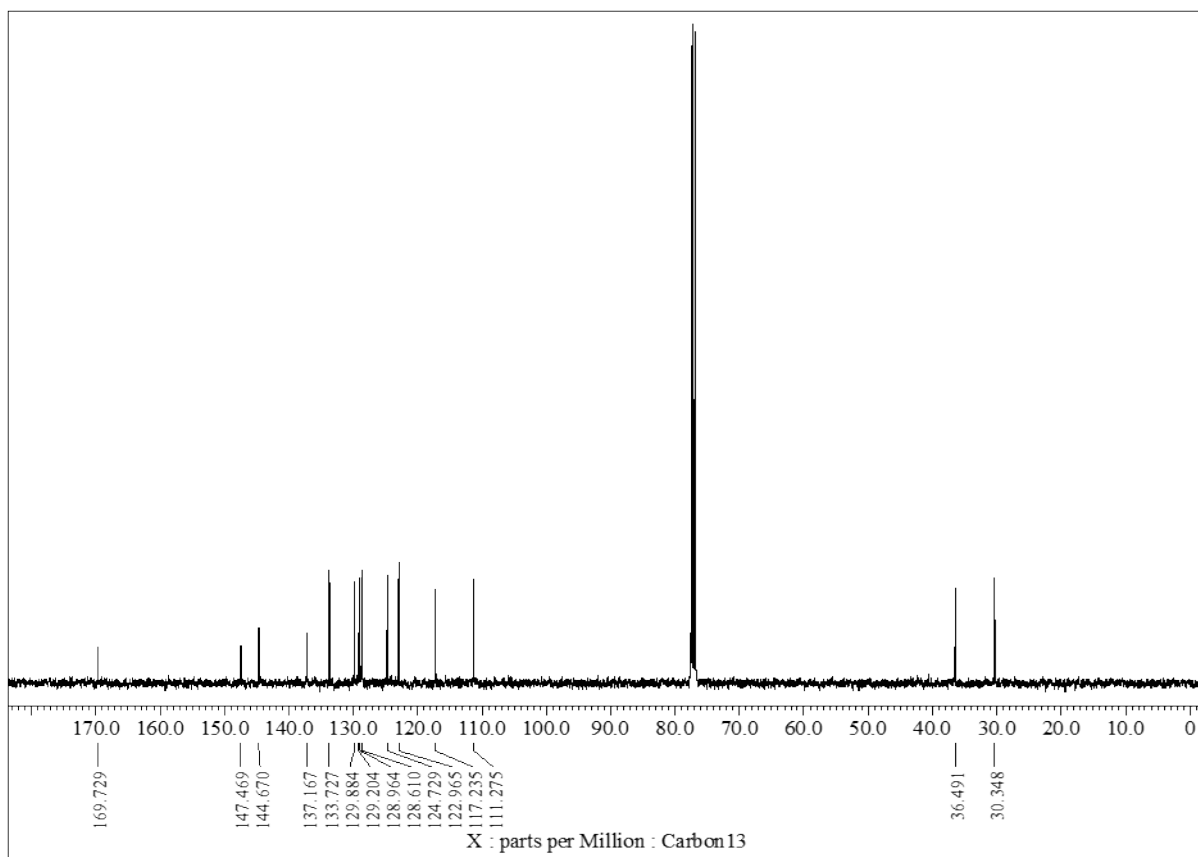


Fig. S15 ¹³C NMR spectrum of NO₂-DMBI-Ox (100 MHz, CDCl₃, 25 °C).